frontiers | Frontiers in Environmental Science

TYPE Brief Research Report
PUBLISHED 22 August 2022
DOI 10.3389/fenvs.2022.965925

OPEN ACCESS

EDITED BY
Bilal Ahmed,
Yeungnam University, South Korea

REVIEWED BY
Muhammad Adeel,
Beijing Normal University, China
Selvaraj Barathi,
Yeungnam University, South Korea
Mohammad Ehtisham Khan,
Jazan University, Saudi Arabia

*CORRESPONDENCE
Adeel Afzal,
aa@aafzal.com
Humaira M. Siddiqi,
humairas@qau.edu.pk

SPECIALTY SECTION
This article was submitted to Toxicology, Pollution and the Environment, a section of the journal Frontiers in Environmental Science

RECEIVED 10 June 2022
ACCEPTED 29 June 2022
PUBLISHED 22 August 2022

CITATION
Faheem M, Siddiqi HM, Habib A, Shahid M and Afzal A (2022), ZnO/$Zn(OH)_2$ nanoparticles and self-cleaning coatings for the photocatalytic degradation of organic pollutants. *Front. Environ. Sci.* 10:965925. doi: 10.3389/fenvs.2022.965925

ZnO/$Zn(OH)_2$ nanoparticles and self-cleaning coatings for the photocatalytic degradation of organic pollutants

Muhammad Faheem[1], Humaira M. Siddiqi[2]*, Amir Habib[3], Muhammad Shahid[4] and Adeel Afzal[4]*

[1]Department of Chemistry, School of Science, University of Management and Technology, Lahore, Pakistan, [2]Department of Chemistry, Quaid-i-Azam University, Islamabad, Pakistan, [3]Department of Physics, College of Science, University of Hafr Al Batin, Hafr Al Batin, Saudi Arabia, [4]Department of Chemistry, College of Science, University of Hafr Al Batin, Hafr Al Batin, Saudi Arabia

Zinc oxide (ZnO) nanostructures have emerged as efficient heterogeneous photocatalysts for the degradation of organic pollutants in aqueous solutions and industrial wastewaters. In this work, a simple and effective method is reported for the synthesis of zinc oxide/zinc hydroxide (ZnO/$Zn(OH)_2$) hybrid nanoparticles using a mineral acid to enhance the photocatalytic activity of ZnO. Infrared spectroscopy reveals the presence of hydroxyl groups in ZnO/$Zn(OH)_2$ nanoparticles. X-ray diffraction shows the formation of hexagonal wurtzite ZnO nanoparticles, which retain their wurtzite structure after acid treatment but additional diffractions for $Zn(OH)_2$ are also recorded. The optical bandgap of resulting ZnO and ZnO/$Zn(OH)_2$ nanoparticles is reduced to 3.05 and 3.08 eV, respectively. In the initial photocatalysis experiments, ZnO/$Zn(OH)_2$ nanoparticles exhibit 3.5-times improved degradation and removal of sunset yellow dye, a model organic pollutant, from deionized water compared to pristine ZnO nanoparticles. Hence, for further studies, ZnO/$Zn(OH)_2$ coatings are fabricated on glass slides with a uniform surface morphology as shown by the atomic force microscopy. The time-dependent UV-visible spectroscopy reveals the photocatalytic degradation of sunset yellow over the surface of ZnO/$Zn(OH)_2$ coatings. The degradation reaction follows the pseudofirst-order mechanism with a rate constant of 2.9×10^{-2} min^{-1}. The recyclability and stability experiments reveal the retention of appreciable photocatalytic activity of ZnO/$Zn(OH)_2$ coatings (with >92% degradation efficiency after six successive cycles). The results are compared with recent examples from the pertinent literature. The surface hydroxyl groups on ZnO/$Zn(OH)_2$ nanoparticles and bandgap lowering enhance the anchoring of dye molecules and electron transfer reactions.

KEYWORDS

dye degradation, photocatalysis, pollution, self-cleaning, sunset yellow, wastewater treatment, ZnO nanoparticles

Introduction

The 20th-century industrial revolution has transformed the lifestyle but deteriorated the environment by polluting the air and aquifers. Industrial wastewaters containing harmful and non-biodegradable organic pollutants such as dyes and pigments (Berradi et al., 2019; Gürses et al., 2021; Orozco et al., 2022), drugs and pharmaceuticals (Akkari et al., 2018; Al-Areqi et al., 2022), etc. Contaminate surface and groundwater sources leading to health risks. Also, the prevalence of organic compounds in the air contaminates surfaces such as textiles and fabrics, glass windows, doors, and other installations, which is often hazardous due to their perilous effects on human health and wellbeing.

To reduce the impact of organic pollutants on the environment and health, photocatalysis–light-induced chemical reactions to oxidize and decompose organic molecules–is developed (Ameta et al., 2018; Zhang et al., 2018). The photoactive nanomaterials can be used as heterogeneous catalysts as well as self-cleaning coatings to remove hazardous organic molecules from the wastewaters (Purcar et al., 2021; Shahid et al., 2021, 2022) or contaminated surfaces (Afzal et al., 2021; Tănase et al., 2021). A variety of nanostructured materials have been developed for the photocatalytic degradation of organic pollutants such as those based on carbon nanostructures (Khan, 2021), titania (Chen et al., 2020; Varma et al., 2020), or zinc oxide (Qi et al., 2017; Majumder et al., 2020).

ZnO is classified as active photocatalysts due to wide absorption range and high photostability (Kołodziejczak-Radzimska and Jesionowski, 2014; Laurenti et al., 2017). Besides, ZnO is harmless and inexpensive, and ZnO nanostructures can be synthesized *via* different methods (Khan et al., 2019a, 2019b; Raha and Ahmaruzzaman, 2022). Qi et al. (Qi et al., 2017) reviewed the photocatalytic applications of ZnO and suggested that the photocatalytic performance of ZnO nanomaterials could be improved by: 1) doping with metals or non-metals, 2) constructing heterojunctions, 3) coupling with carbon nanostructures, or 4) deposition of noble metals. For instance, Ag doping is shown to improve the photocatalytic degradation of both cationic and anionic dyes under simulated solar irradiation by Ag@ZnO nanocomposites (Sharwani et al., 2022).

However, these methods generally involve the addition of other active components in ZnO to enhance its photoactivity. Herein, a simple and effective method is used to improve the photocatalytic properties of ZnO nanoparticles that employs a mineral acid treatment to protonate ZnO surfaces and improve dye adsorption and degradation. Previously, acid treatment of TiO_2-based photocatalyst and its influence on the degradation of organic dyes have been studied (Park and Shin, 2014). For instance, Dhandole et al. (Dhandole et al., 2017) suggested that acid treatment of Co_2O_3-TiO_2 nanorods exhibited a higher efficiency for the photocatalytic degradation of orange-II dye. However, contrary to these findings, Onoda et al. (Onoda, 2019) recently reported that phosphoric acid treatment was detrimental to the photocatalytic activity of ZnO.

This work is aimed at studying the effects of a mineral acid treatment of ZnO on its photocatalytic properties. For this purpose, ZnO nanoparticles are prepared and treated with 1.0 M HCl to form ZnO/$Zn(OH)_2$ hybrid nanoparticles and coatings, which are subsequently used for the degradation of organic pollutants in deionized water. As a model organic compound, sunset yellow dye is chosen because of its carcinogenicity and non-biodegradability (Sharma et al., 2020). ZnO/$Zn(OH)_2$ nanoparticles and coatings are characterized and tested for their photocatalytic activity. Hexagonal wurtzite ZnO/$Zn(OH)_2$ coatings exhibit excellent photocatalytic properties by oxidizing and removing sunset yellow. The coatings are stable over several cycles of photocatalytic measurements in aqueous solutions.

Methods

Synthesis

ZnO nanoparticles were synthesized by the precipitation method using zinc nitrate hexahydrate ($Zn(NO_3)_2.6H_2O$ purum p.a., crystallized, ≥99.0%, SigmaAldrich) as a precursor, and ethanolamine (≥98.0%, SigmaAldrich) as the solvent as well as the surfactant (Naz et al., 2015). Firstly, 20 ml distilled ethanolamine was taken in a 250 ml round bottom flask. 14 mmol of $Zn(NO_3)_2.6H_2O$ were added to it and stirred at room temperature until a clear solution was obtained. The solution was transparent with no turbidity. Then 10 ml of ammonia solution (NH_4OH, 32%, EMPLURA®, SigmaAldrich) was added dropwise to the transparent precursor solution to attain the basic pH (pH ~ 11). The solution was allowed to stir at 60°C for 60 min. During this period, white precipitates of ZnO nanoparticles were produced. The product was centrifuged, washed with an excess of distilled water, and dried in an oven at 100°C. The yield of the final product, i.e., ZnO nanoparticles in dried powdered form was 24.2%.

ZnO/$Zn(OH)_2$ nanoparticles were produced by surface protonation of the as-synthesized ZnO nanoparticles. For this purpose, as-synthesized ZnO nanoparticles were dispersed in an excess of 1 M aqueous HCl, and the suspension was kept in an ultrasonic bath for an hour at room temperature. Afterward, the mixture was centrifuged to separate ZnO/$Zn(OH)_2$ nanoparticles, which were washed with distilled water, and dried in an oven at 100°C. Both ZnO and ZnO/$Zn(OH)_2$ nanoparticles were characterized and tested for their photocatalytic properties.

Characterization

Fourier-transform infrared (FTIR) spectroscopy of solid ZnO and $ZnO/Zn(OH)_2$ nanoparticles was performed with Thermo Scientific Nicolet 6700 FTIR spectrophotometer in the range of 4000–400 cm^{-1}. X-ray diffraction (XRD) patterns were obtained with a Siemens D–5000 XRD system utilizing a Cu Kα radiation source (λ = 1.5406 Å). Ultraviolet-visible (UV-vis) spectroscopy was carried out with the Shimadzu model pharma spec UV–1700 UV-vis spectrophotometer in the range of 200–800 nm. The cuvettes used were made up of quartz by Shimadzu.

The surface morphology of $ZnO/Zn(OH)_2$ coatings on the glass slide was examined by Shimadzu WET-SPM 9600 atomic force microscope (AFM) using the contact mode. WSxM 4.0 Beta 9.3 scanning probe microscopy software was used for image analysis and calculation of surface parameters (Horcas et al., 2007).

Photocatalytic performance: Degradation of organic pollutants

The photocatalytic properties of ZnO and $ZnO/Zn(OH)_2$ nanoparticles were studied by the light-induced degradation of sunset yellow (a model organic contaminant) at 25°C. First, a solution of sunset yellow (20 μg mL^{-1}) was prepared. Sunset yellow dye shows good stability to changes in pH and it does not exhibit an appreciable change within the pH range of 3–8. Hence, the dye solutions were maintained at pH 6 for all experiments. ZnO or $ZnO/Zn(OH)_2$ nanoparticles (1 mg mL^{-1}) were dispersed in the solution and it was kept in dark for an hour to establish the adsorption-desorption equilibrium. After an hour, the absorption spectra of the dye solutions were recorded with a UV-vis spectrophotometer. Subsequently, the solutions were exposed to UV light (λ = 365 nm) for 2 h. The optimal distance between the solutions and the UV light source was maintained at 20 cm to avoid the heating effect. Afterward, the UV-vis spectra of the same solutions were recorded again to compare the absorbance and photocatalytic performance of ZnO and $ZnO/Zn(OH)_2$ nanoparticles were estimated.

$ZnO/Zn(OH)_2$ coatings for pollutant degradation

Self-cleaning $ZnO/Zn(OH)_2$ coatings were prepared on glass slides (1 cm × 2 cm) *via* spray coating a suspension of nanoparticles in 4 wt% poly(vinyl acetate). The glass slides were first cleaned in an ultrasonic bath with acetone, methanol, and deionized water for 5 min, respectively. Subsequently, three aliquots of $ZnO/Zn(OH)_2$ nanoparticles were spray-coated and air-dried at room temperature. These coatings were subsequently exposed to organic contaminants in a solution to study their photodegradation performance.

For $ZnO/Zn(OH)_2$ coatings, photocatalytic activity was explored by studying the degradation of sunset yellow under 365 nm light illumination at 25°C. $ZnO/Zn(OH)_2$ samples with a size of 1 cm × 2 cm were immersed into a 70 ml dye solution (20 μg mL^{-1}). The solution was stirred in dark for an hour to develop an adsorption-desorption equilibrium. Afterward, the dye solution with $ZnO/Zn(OH)_2$ sample was exposed to UV irradiation for 0–120 min. During this period, the absorption spectrum of the sunset yellow solution was recorded at 0 min exposure to UV light (as the initial reading), and subsequently, the absorbance was measured after every 15 min of UV exposure in the range of 325–600 nm. To determine the recyclability and stability of $ZnO/Zn(OH)_2$ coatings on glass, the photocatalytic performance was repeatedly measured under similar conditions, i.e. at 25°C and 365 nm UV illumination.

Results and discussion

Characterization

The formation of ZnO and $ZnO/Zn(OH)_2$ is depicted in Figure 1A. ZnO is prepared *via* an ethanolamine-mediated precipitation of ZnO from a $Zn(NO_3)_2$ solution using NH_4OH. Ethanolamine simultaneously acts as a solvent and a surfactant (Naz et al., 2015). ZnO nanoparticles are subsequently treated with an acid to protonate the surface oxygens and form a hybrid $ZnO/Zn(OH)_2$ structure with surface hydroxyl groups. Wang et al. (Wang et al., 2005) already demonstrated a straightforward and effective method for proton adsorption on the surface of TiO_2 films that was based on acid (0.1 M HCl) treatment.

Figure 1B shows the FTIR spectra of ZnO and $ZnO/Zn(OH)_2$ nanoparticles, which are markedly different in terms of the presence of–OH groups. As-synthesized ZnO nanoparticles show the characteristic Zn–O vibration at ~400 and 421 cm^{-1} (Estrada-Urbina et al., 2018). FTIR spectrum of $ZnO/Zn(OH)_2$ nanoparticles, on the other hand, confirms the presence of hydroxyl moieties (–OH groups) along with the characteristic Zn–O vibrations (~400 (Estrada-Urbina et al., 2018), 421, and 458 cm^{-1} (Handore et al., 2014)). A broad absorption peak with a maximum at 3,440 cm^{-1} corresponds to the stretching vibrations of O–H groups located on the surface of $ZnO/Zn(OH)_2$ nanoparticles (Hadjiivanov, 2014). The appearance of additional peaks around 1499 and 916 cm^{-1} is also attributed to the formation of $Zn(OH)_2$ (Khanom and Hayashi, 2021), while the absorption bands around 1380 and 880 cm^{-1} are ascribed to the adsorbed CO_2 (Estrada-Urbina et al., 2018).

XRD patterns of ZnO and $ZnO/Zn(OH)_2$ nanoparticles between 10° and 80° 2θ are presented in Figure 1C. The main diffraction peaks correspond to the hexagonal wurtzite ZnO

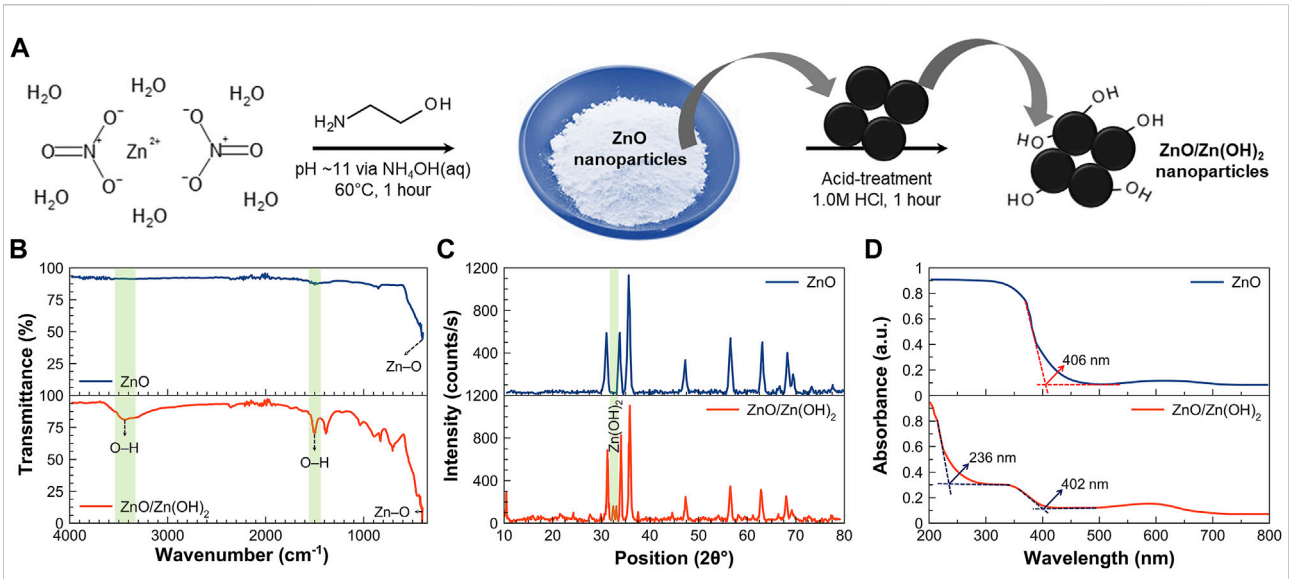

FIGURE 1
(A) A schematic showing the formation of ZnO and ZnO/$Zn(OH)_2$ nanoparticles. **(B)** Fourier-transform infrared spectra, **(C)** X-ray diffraction patterns, and **(D)** UV-vis spectra of ZnO and ZnO/$Zn(OH)_2$ nanoparticles showing the notable differences in the molecular and crystalline structure of pristine ZnO and composite ZnO/$Zn(OH)_2$ nanoparticles and their optical properties.

crystal structure with space group $P6_3mc$ and can be correlated with JCPDS 36–1451 (Singh, 2011). The characteristic diffraction peaks of ZnO nanoparticles appear at 31.6°, 34.3°, 36.1°, 47.4°, 56.4°, 62.6°, and 67.9° 2θ and correspond to the (100), (002), (101), (102), (110), (103), and (112) miller indices, respectively. The diffraction pattern of ZnO/$Zn(OH)_2$ nanoparticles is quite similar to ZnO, which shows the hexagonal wurtzite ZnO as the major crystalline phase. However, compared to pristine ZnO, ZnO/$Zn(OH)_2$ nanoparticles exhibit additional peaks at 2θ = 32.8° (Emara et al., 2021) and 33.5° (Molefe et al., 2015), corresponding to $Zn(OH)_2$.

The respective lattice parameters for ZnO and ZnO/$Zn(OH)_2$ nanoparticles are determined from the XRD data, and are comparable as follows: $a = b = 3.26$ Å (ZnO) and 3.24 Å (ZnO/$Zn(OH)_2$); and $c = 5.21$ Å (ZnO) and 5.16 Å (ZnO/$Zn(OH)_2$). These lattice parameters are consistent with the values reported in the literature (Awan et al., 2018). The crystallite size is determined by Debye–Scherer's formula (Afzal et al., 2020). The average crystallite size of the ZnO and ZnO/$Zn(OH)_2$ nanoparticles is found to be 16.6 and 18.0 nm, respectively. The density (ρ) and the specific surface area (SSA) of the ZnO and ZnO/$Zn(OH)_2$ nanoparticles are also estimated from XRD data, which are as follows: ZnO nanoparticles ($\rho = 16.08$ g cm^{-3}; SSA = 22.48 m^2 g^{-1}), and ZnO/$Zn(OH)_2$ nanoparticles ($\rho = 16.41$ g cm^{-3}; SSA = 20.31 m^2 g^{-1}).

UV-vis spectra of ZnO and ZnO/$Zn(OH)_2$ nanoparticles are recorded in Figure 1D. On basis of the intersection along the baseline (Lin et al., 2011), ZnO and ZnO/$Zn(OH)_2$ nanoparticles absorb at 406 and 402 nm, respectively. The absorbance (ca. 406–402 nm) corresponds to the optical bandgap of 3.05–3.08 eV for ZnO and ZnO/$Zn(OH)_2$ nanoparticles, which is significantly less than the direct bandgap of bulk ZnO, i.e., 3.37 eV (Kamarulzaman et al., 2015). A reduction in the bandgap of ZnO and ZnO/$Zn(OH)_2$ nanoparticles compared to that of bulk ZnO and a significant shift in the near violet region may be attributed to the quantum confinement effect (Kumar et al., 2017). A clear difference in the UV-vis spectra of ZnO and ZnO/$Zn(OH)_2$ nanoparticles is the secondary absorbance at ~236 nm that is attributed to the presence of the $Zn(OH)_2$ phase. This wavelength corresponds to the direct bandgap of 5.3 eV, which is in agreement with the bandgap of $Zn(OH)_2$ (Wang et al., 2015).

Photocatalytic degradation of sunset yellow: Preliminary experiments

The preliminary experiments performed for the assessment of the photocatalytic performance of ZnO and ZnO/$Zn(OH)_2$ nanoparticles involved the degradation of sunset yellow after 2 h of light irradiation. The aqueous solutions of 20 μg mL^{-1} sunset yellow containing 1 mg mL^{-1} of ZnO and ZnO/$Zn(OH)_2$ nanoparticles were exposed to UV light after the establishment of adsorption-desorption equilibrium. The degradation of sunset yellow was monitored with a UV-vis spectrophotometer. Figure 2A shows the photocatalytic degradation performance of ZnO and ZnO/$Zn(OH)_2$ nanoparticles. After 2 h of light exposure, the dye is almost

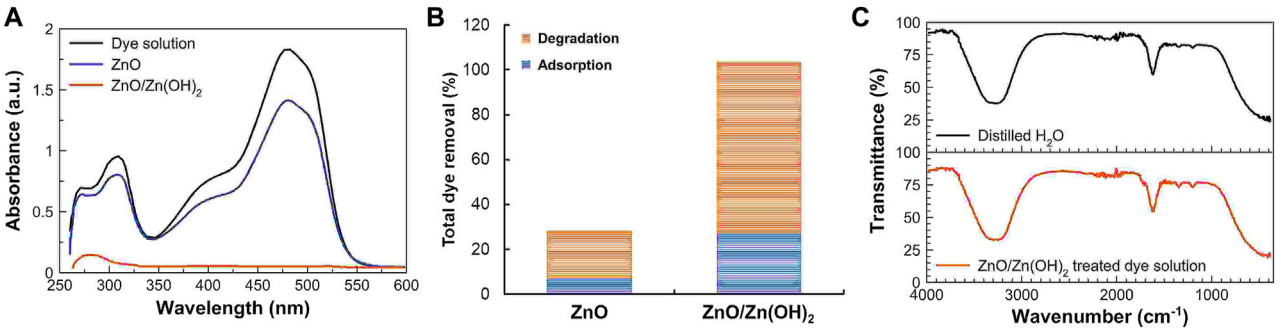

FIGURE 2
(A) UV-vis spectra of the aqueous solution of sunset yellow and its exposure to UV light in the presence of ZnO and $ZnO/Zn(OH)_2$ nanoparticles. **(B)** The overall dye removal shows the photocatalytic degradation performance of ZnO and $ZnO/Zn(OH)_2$ nanoparticles. **(C)** FTIR spectra of the distilled H_2O and $ZnO/Zn(OH)_2$ nanoparticles treated dye solution.

completely removed by $ZnO/Zn(OH)_2$ nanoparticles, while pristine ZnO nanoparticles did not exhibit comparable photocatalytic activity.

The analysis of UV-vis spectra before and after adsorption-desorption and after 2 h of light exposure shows that the overall dye removal by $ZnO/Zn(OH)_2$ (97.4%) was 3.5-fold higher than ZnO nanoparticles (28.2%), as shown in Figure 2B. Also, $ZnO/Zn(OH)_2$ nanoparticles adsorbed a significantly greater amount of sunset yellow (27.3%) compared to ZnO nanoparticles (7.1%). This is because of the presence of surface hydroxyl (–OH) groups, which may develop non-covalent interactions with the sunset yellow molecule. Consequently, in turn, the photocatalytic processes are supported by the enhanced adsorption of the dye molecules (Paul et al., 2020).

However, the degradation of sunset yellow is not merely the decolorization of dye solution. To investigate the persistence of degraded organic products in the sunset yellow solution treated with $ZnO/Zn(OH)_2$ nanoparticles, its FTIR spectrum was recorded and compared with the spectrum of distilled water as shown in Figure 2C. Before recording the FTIR spectrum of $ZnO/Zn(OH)_2$ nanoparticles treated dye solution, the solution was centrifuged to remove $ZnO/Zn(OH)_2$ nanoparticles. Both of these FTIR spectra, shown in Figure 2C, were similar, and no additional peaks for the organic species or functional groups were observed. It indicated that sunset yellow molecules were completely degraded into non-toxic components such as water and carbon dioxide.

Pollutant degradation by $ZnO/Zn(OH)_2$ coatings

From the preliminary experiments on the photocatalytic performance of solid ZnO and $ZnO/Zn(OH)_2$ nanoparticles, it is confirmed that $ZnO/Zn(OH)_2$ nanoparticles exhibit superior photocatalytic properties compared to pristine ZnO. Hence, only $ZnO/Zn(OH)_2$ nanoparticles were tested further as photocatalytic coatings for pollutant degradation applications.

$ZnO/Zn(OH)_2$ coatings were fabricated on glass slides *via* spray coating. Figure 3 shows the surface analysis of $ZnO/Zn(OH)_2$ coatings. Two- and three-dimensional micrographs and phase images demonstrate the surface morphology of the coatings with the consistent presence of $ZnO/Zn(OH)_2$ nanoparticles on the glass surface. The root-mean-square (*RMS*) roughness and the average surface roughness are recorded as 75.47 and 59.04 nm, respectively with an average height of 172.82 nm. The surface profiles and particles' size distribution histogram are consistent with the roughness analysis and calculated values.

The photocatalytic properties of the $ZnO/Zn(OH)_2$ coating were measured by the degradation of sunset yellow in water under UV light illumination. The time-dependent percent degradation of sunset yellow was calculated as follows (Islam et al., 2019):

$$\textit{degradation}\ (\%) = \left(\frac{(A_o - A_t)}{A_o}\right) \times 100 = \left(\frac{(C_o - C_t)}{C_o}\right) \times 100$$

where A_o and A_t correspond to the initial absorbance at $t = 0$ min and time-dependent absorbance of sunset yellow after UV light irradiation, respectively; and C_o and C_t are the respective concentrations of sunset yellow. UV-vis spectroscopy was used to study the degradation of sunset yellow. The time-dependent UV-vis spectra of 20 ppm sunset yellow solution in deionized water are presented in Figure 4A which exhibit its photocatalytic degradation in the presence of $ZnO/Zn(OH)_2$ coatings. The absorbance (A_t/A_o) of the sunset yellow solution is plotted as a function of time in Figure 4B. As revealed in Figures 4A,B, the concentration of sunset yellow solution regularly decreases with the UV irradiation time due to the

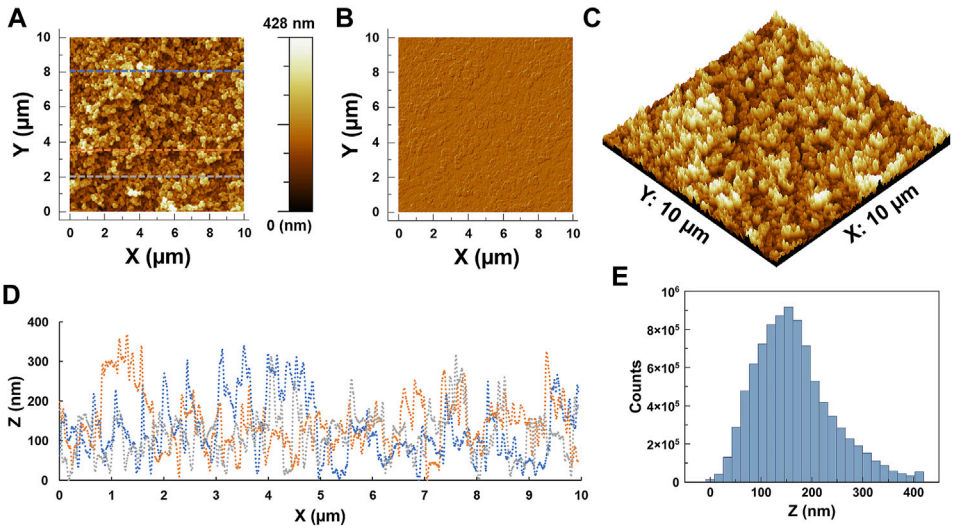

FIGURE 3
Atomic force microscopy of ZnO/Zn(OH)$_2$ coatings fabricated on glass slides: **(A)** A topography image, and corresponding **(B)** phase image, **(C)** 3-dimensional topography map, **(D)** surface profiles, and **(E)** surface roughness analysis histogram.

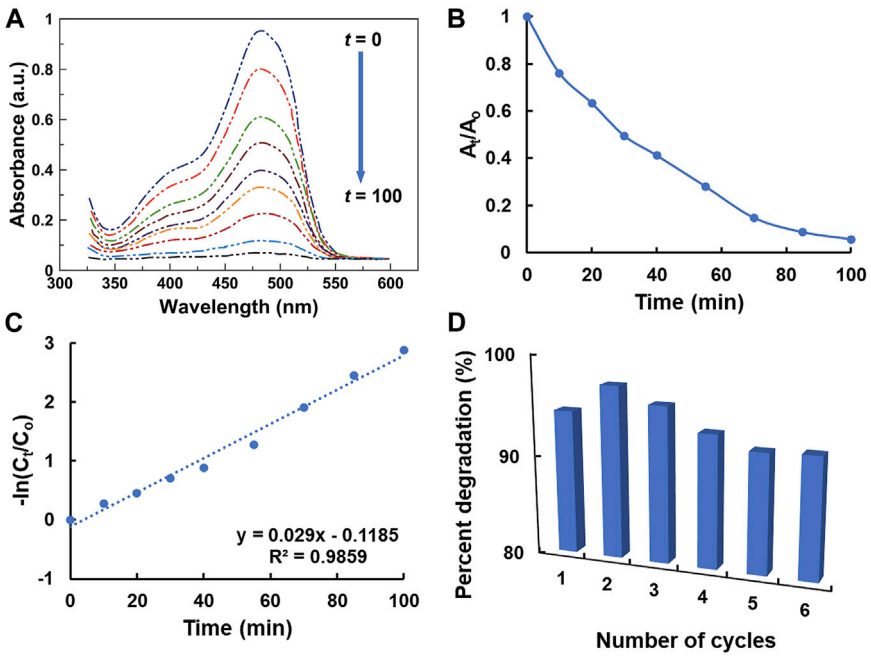

FIGURE 4
(A) The time-dependent photocatalytic performance of ZnO/Zn(OH)$_2$ coatings: UV-vis spectra of the sunset yellow solution at different intervals (t = 0–100 min) of UV light (λ = 365 nm) irradiation. **(B)** A relationship of the initial (A_o) and time-dependent (A_t) absorbance of sunset yellow with UV irradiation time (t). **(C)** A kinetics analysis: pseudofirst-order kinetics ($-ln(C_t/C_o)$ vs. t) of the photocatalytic degradation of sunset yellow. **(D)** Recyclability of the photocatalytic ZnO/Zn(OH)$_2$ coatings.

TABLE 1 A comparison of the photodegradation of sunset yellow by various nanostructured photocatalysts.

Photocatalyst	Band-gap (eV)	Catalyst dose (mg ml^{-1})	Dye concentration (μM)	pH	Rate of degradation (min^{-1})	Reusability[1] (%)	References
$ZnO/Zn(OH)_2$	3.08	1.0	44.2	6.0	2.9×10^{-2}	95.56	This work
Chitosan/ZnSe	—	3.0	44.2	5.0	4.317×10^{-2}	82.42	Zhang et al. (2022)
Pd–$BiFeO_3$	2.23	1.5	22.1	—	1.688×10^{-2}	~98	Jaffari et al. (2021)
Se nanoparticles	2.3	0.3	11	5.8	1.73×10^{-1}	—	Hassanien et al. (2019)
SeO_2/TiO_2	2.9	5.0	300	7.0	3.06×10^{-2}	94.6	Rajamanickam et al. (2015)
Activated carbon/ TiO_2	—	4.0	300	7.0	—	96.4	Rajamanickam and Shanthi, (2014)

[1]Reusability refers to the percent degradation of sunset yellow dye after 3 successive cycles.

photocatalytic effect of $ZnO/Zn(OH)_2$ coatings. The absorption maxima around 400 and 480 nm gradually disappear after 100 min of exposure to UV light, which suggests the complete degradation of sunset yellow in water.

The experimentally observed photocatalytic degradation properties of $ZnO/Zn(OH)_2$ coatings were further explored by the pseudofirst-order kinetic model. The kinetics of photocatalytic degradation was measured by the following apparent pseudofirst-order rate equation:

$$-ln(C_t/C_o) = kt$$

where k is the rate constant, and t is the UV irradiation time. The relation between $-ln(C_t/C_o)$ and t is plotted in Figure 4C. As shown in Figure 4C, the $-ln(C_t/C_o)$ versus t graph reveals the linear trend with $R^2 = 0.986$, which indicates that the sunset yellow degradation proceeds *via* the pseudofirst-order reaction mechanism and follows the Langmuir–Hinshelwood model (Khezrianjoo and Revanasiddappa, 2012; Moghaddas et al., 2020). The rate constant (k) for the photocatalytic degradation of sunset yellow is calculated to be 2.9×10^{-2} min^{-1} (standard deviation: $\pm 1.3 \times 10^{-3}$ min^{-1}) for 20 ppm sunset yellow in deionized water.

The recyclability and stability of $ZnO/Zn(OH)_2$ coatings on glass were determined by repeated photocatalysis experiments at 25°C. The results are recorded in Figure 4D. As shown in Figure 4D, the percent degradation of sunset yellow in deionized water after UV illumination of $ZnO/Zn(OH)_2$ coatings for six different cycles are comparable, and above 92% after several cycles. The mean value for the percent degradation of sunset yellow after six measurements is 94.0%, and the standard deviation is ±1.9%.

The photocatalytic performance of $ZnO/Zn(OH)_2$ coatings is compared with various other photocatalysts reported in the past few years and the data are represented in Table 1. $ZnO/Zn(OH)_2$ coatings exhibit excellent photocatalytic properties toward sunset yellow degradation. Based on the experimental observations, the enhanced photocatalytic properties of the $ZnO/Zn(OH)_2$ coatings are attributed to the presence of surface hydroxyl groups and the narrow bandgap, which result in the improved interactions between the $ZnO/Zn(OH)_2$ coatings and sunset yellow molecules and greater electron transfer speed for the degradation reaction. Given the high photocatalytic activity, recyclability, and stability of $ZnO/Zn(OH)_2$ coatings, they have potential applications in the light-induced catalytic degradation of organic pollutants in the wastewater as well as self-cleaning coatings and surfaces for environmental and industrial applications.

Conclusion

ZnO nanoparticles were prepared *via* a simple aminoethanol-mediated precipitation of $Zn(NO_3)_2$ solution with aqueous NH_3. Pristine ZnO nanoparticles were subsequently treated with a mineral acid to form $ZnO/Zn(OH)_2$ hybrid nanoparticles. Both ZnO and $ZnO/Zn(OH)_2$ nanoparticles were characterized by XRD, FTIR, and UV-vis spectroscopy. The XRD analysis revealed the formation of hexagonal wurtzite ZnO and $ZnO/Zn(OH)_2$ nanoparticles. $ZnO/Zn(OH)_2$ nanoparticles additionally exhibited the presence of $Zn(OH)_2$ phases in XRD, and surface hydroxyl groups in the FTIR spectrum. UV-vis spectroscopy revealed significant lowering of the optical bandgap to ~3.1 eV. The preliminary photocatalysis experiments confirmed that $ZnO/Zn(OH)_2$ nanoparticles possessed superior photocatalytic properties toward the degradation of sunset yellow, a model organic pollutant, in deionized water. $ZnO/Zn(OH)_2$ nanoparticles treatment under UV irradiation completely degraded the sunset yellow molecules, and the persistence of organic species in treated solution was not observed. The bandgap narrowing and surface hydroxyl groups were the reasons for the improved photocatalytic activity of $ZnO/Zn(OH)_2$ nanoparticles. $ZnO/Zn(OH)_2$ coatings were also fabricated and tested for their photocatalytic performance and stability, which demonstrated pseudofirst-order degradation

kinetics with a rate constant of 2.9×10^{-2} min^{-1}, and excellent stability after 6 cycles of photocatalytic degradation while maintaining more than 92% degradation of sunset yellow. The results were compared with the recent literature on photocatalytic degradation of sunset yellow. The results indicate the potential of $ZnO/Zn(OH)_2$ coatings in self-cleaning and environmental applications for pollutant degradation.

Data availability statement

The original contributions presented in the study are included in the article/Supplementary material, further inquiries can be directed to the corresponding author.

Author contributions

Conceptualization, HS and AA; methodology, MF; validation, MF, AH, and MS; formal analysis, MF and AH; investigation, MF; resources, HS and AA; data curation, MF and AA; writing—original draft preparation, AA; writing—review and editing, HS and M.S.; visualization, AH; supervision, HS; project administration, AA; funding acquisition, AA All authors have read and agreed to the published version of the manuscript.

Funding

The authors extend their appreciation to the Deputyship for Research and Innovation, Ministry of Education in Saudi Arabia for funding this research work through the project number IFP-A-202-1-1.

Acknowledgments

AA gratefully acknowledges the financial support provided by the Agency for Research and Innovation, Ministry of Education in Saudi Arabia through the project number IFP-A-202-1-1. AA also appreciates the assistance received from the Department of Chemistry, Quaid-i-Azam University (Pakistan) and the Deanship of Scientific Research, University of Hafr Al Batin (Saudi Arabia) to perform this work. HMS acknowledges the University Research Fund, Quaid-i-Azam University (Pakistan) for continuous support.

Conflict of interest

The authors declare that the research was conducted in the absence of any commercial or financial relationships that could be construed as a potential conflict of interest.

Publisher's note

All claims expressed in this article are solely those of the authors and do not necessarily represent those of their affiliated organizations, or those of the publisher, the editors and the reviewers. Any product that may be evaluated in this article, or claim that may be made by its manufacturer, is not guaranteed or endorsed by the publisher.

References

Afzal, A., Abuilaiwi, F. A., Javaid, R., Ali, F., and Habib, A. (2020). Solid-state synthesis of heterogeneous Ni0.5Cu0.5-xZnxFe2O4 spinel oxides with controlled morphology and tunable dielectric properties. *J. Mater. Sci. Mater. Electron.* 31, 14261–14270. doi:10.1007/s10854-020-03982-8

Afzal, A., Habib, A., Ulhasan, I., Shahid, M., and Rehman, A. (2021). Antireflective self-cleaning TiO2 coatings for solar energy harvesting applications. *Front. Mater.* 8, 205. doi:10.3389/fmats.2021.687059

Akkari, M., Aranda, P., Belver, C., Bedia, J., Ben Haj Amara, A., Ruiz-Hitzky, E., et al. (2018). ZnO/sepiolite heterostructured materials for solar photocatalytic degradation of pharmaceuticals in wastewater. *Appl. Clay Sci.* 156, 104–109. doi:10.1016/j.clay.2018.01.021

Al-Areqi, N. A. S., Umair, M., Senan, A. M., Al-Alas, A., Alfaatesh, A. M. A., Beg, S., et al. (2022). Mesoporous nano-sized BiFeVOx.y phases for removal of organic dyes from wastewaters by visible light photocatalytic degradation. *Nanomaterials* 12, 1383. doi:10.3390/nano12081383

Ameta, R., Solanki, M. S., Benjamin, S., and Ameta, S. C. (2018). "Chapter 6 - photocatalysis," in *Advanced oxidation processes for waste water treatment*. Editors S. C. Ameta and R. Ameta (Academic Press), 135–175. doi:10.1016/B978-0-12-810499-6.00006-1

Awan, S. U., Hasanain, S. K., Rashid, J., Hussain, S., Shah, S. A., Hussain, M. Z., et al. (2018). Structural, optical, electronic and magnetic properties of multiphase ZnO/Zn(OH)2/ZnO2 nanocomposites and hexagonal prism shaped ZnO nanoparticles synthesized by pulse laser ablation in Heptanes. *Mater. Chem. Phys.* 211, 510–521. doi:10.1016/j.matchemphys.2018.02.051

Berradi, M., Hsissou, R., Khudhair, M., Assouag, M., Cherkaoui, O., El Bachiri, A., et al. (2019). Textile finishing dyes and their impact on aquatic environs. *Heliyon* 5, e02711. doi:10.1016/j.heliyon.2019.e02711

Chen, D., Cheng, Y., Zhou, N., Chen, P., Wang, Y., Li, K., et al. (2020). Photocatalytic degradation of organic pollutants using TiO2-based photocatalysts: A review. *J. Clean. Prod.* 268, 121725. doi:10.1016/j.jclepro.2020.121725

Dhandole, L. K., Mahadik, M. A., Kim, S.-G., Chung, H.-S., Seo, Y.-S., Cho, M., et al. (2017). Boosting photocatalytic performance of inactive rutile TiO2 nanorods under solar light irradiation: Synergistic effect of acid treatment and metal oxide Co-catalysts. *ACS Appl. Mater. Interfaces* 9, 23602–23613. doi:10.1021/acsami.7b02104

Emara, M. M., Ragab, D. M., and Kassem, T. S. E. (2021). Deposition of ZnS dots onto nanosheets of cobalt-doped ZnO–Zn(OH)2 and their photocatalytic activity. *J. Phys. Chem. Solids* 148, 109702. doi:10.1016/j.jpcs.2020.109702

Estrada-Urbina, J., Cruz-Alonso, A., Santander-González, M., Méndez-Albores, A., and Vázquez-Durán, A. (2018). Nanoscale zinc oxide particles for improving the physiological and sanitary quality of a Mexican landrace of red maize. *Nanomaterials* 8, 247. doi:10.3390/nano8040247

Gürses, A., Güneş, K., and Şahin, E. (2021). "Chapter 5 - removal of dyes and pigments from industrial effluents," in *Green Chemistry and water remediation:*

Research and applications. Advances in green and sustainable Chemistry. Editor S. K. Sharma (Elsevier), 135–187. doi:10.1016/B978-0-12-817742-6.00005-0

Hadjiivanov, K. (2014). "Identification and characterization of surface hydroxyl groups by infrared spectroscopy," in *Advances in catalysis*. Editor F. C. Jentoft (Academic Press), 99–318. doi:10.1016/B978-0-12-800127-1.00002-3

Handore, K., Bhavsar, S., Horne, A., Chhattise, P., Mohite, K., Ambekar, J., et al. (2014). Novel green route of synthesis of ZnO nanoparticles by using natural biodegradable polymer and its application as a catalyst for oxidation of aldehydes. *J. Macromol. Sci. Part A* 51, 941–947. doi:10.1080/10601325.2014.967078

Hassanien, R., Abed-Elmageed, A. A. I., and Husein, D. Z. (2019). Eco-friendly approach to synthesize selenium nanoparticles: Photocatalytic degradation of sunset yellow azo dye and anticancer activity. *ChemistrySelect* 4, 9018–9026. doi:10.1002/slct.201901267

Horcas, I., Fernández, R., Gómez-Rodríguez, J. M., Colchero, J., Gómez-Herrero, J., Baro, A. M., et al. (2007). WSXM: A software for scanning probe microscopy and a tool for nanotechnology. *Rev. Sci. Instrum.* 78, 013705. doi:10.1063/1.2432410

Islam, T., Md., Dominguez, A., Alvarado-Tenorio, B., Bernal, R. A., Montes, M. O., Noveron, J. C., et al. (2019). Sucrose-mediated fast synthesis of zinc oxide nanoparticles for the photocatalytic degradation of organic pollutants in water. *ACS Omega* 4, 6560–6572. doi:10.1021/acsomega.9b00023

Jaffari, Z. H., Lam, S. M., Ng, D. Q., and Sin, J. C. (2021). Visible light photocatalytic degradation of sunset yellow dye and industrial textile wastewater using Pd-BiFeO3 composite. *IOP Conf. Ser. Earth Environ. Sci.* 835, 012001. doi:10.1088/1755-1315/835/1/012001

Kamarulzaman, N., Kasim, M. F., and Rusdi, R. (2015). Band gap narrowing and widening of ZnO nanostructures and doped materials. *Nanoscale Res. Lett.* 10, 346. doi:10.1186/s11671-015-1034-9

Khan, M. M., Saadah, N. H., Khan, M. E., Harunsani, M. H., Tan, A. L., Cho, M. H., et al. (2019a). Phytogenic synthesis of band gap-narrowed ZnO nanoparticles using the bulb extract of Costus woodsonii. *Bionanoscience* 9, 334–344. doi:10.1007/s12668-019-00616-0

Khan, M. M., Saadah, N. H., Khan, M. E., Harunsani, M. H., Tan, A. L., Cho, M. H., et al. (2019b). Potentials of Costus woodsonii leaf extract in producing narrow band gap ZnO nanoparticles. *Mater. Sci. Semicond. Process.* 91, 194–200. doi:10.1016/j.mssp.2018.11.030

Khan, M. E. (2021). State-of-the-art developments in carbon-based metal nanocomposites as a catalyst: photocatalysis. *Nanoscale Adv.* 3, 1887–1900. doi:10.1039/D1NA00041A

Khanom, S., and Hayashi, N. (2021). Removal of metal ions from water using oxygen plasma. *Sci. Rep.* 11, 9175. doi:10.1038/s41598-021-88466-3

Khezrianjoo, S., and Revanasiddappa, H. D. (2012). Langmuir-Hinshelwood kinetic expression for the photocatalytic degradation of metanil yellow aqueous solutions by ZnO catalyst. *Chem. Sci. J.* Available at: link.gale.com/apps/doc/A335292551/AONE?u=anon~9e6aeef0&sid=googleScholar&xid=ab80d995 (Accessed May 1, 2022).

Kołodziejczak-Radzimska, A., and Jesionowski, T. (2014). Zinc oxide—from synthesis to application: A review. *Materials* 7, 2833–2881. doi:10.3390/ma7042833

Kumar, Y., Kumar, H., Rawat, G., Kumar, C., Sharma, A., Pal, B. N., et al. (2017). Colloidal ZnO quantum dots based spectrum selective ultraviolet photodetectors. *IEEE Photonics Technol. Lett.* 29, 361–364. doi:10.1109/LPT.2016.2647321

Laurenti, M., Stassi, S., Canavese, G., and Cauda, V. (2017). Surface engineering of nanostructured ZnO surfaces. *Adv. Mater. Interfaces* 4, 1600758. doi:10.1002/admi.201600758

Lin, B. C., Shen, P., and Chen, S. Y. (2011). ZnO and ε-Zn(OH)2 composite nanoparticles by pulsed laser ablation on Zn in water. *J. Phys. Chem. C* 115, 5003–5010. doi:10.1021/jp107140r

Majumder, S., Chatterjee, S., Basnet, P., and Mukherjee, J. (2020). ZnO based nanomaterials for photocatalytic degradation of aqueous pharmaceutical waste solutions–A contemporary review. *Environ. Nanotechnol. Monit. Manag.* 14, 100386. doi:10.1016/j.enmm.2020.100386

Moghaddas, S. M. T. H., Elahi, B., and Javanbakht, V. (2020). Biosynthesis of pure zinc oxide nanoparticles using Quince seed mucilage for photocatalytic dye degradation. *J. Alloys Compd.* 821, 153519. doi:10.1016/j.jallcom.2019.153519

Molefe, F. V., Koao, L. F., Dejene, B. F., and Swart, H. C. (2015). Phase formation of hexagonal wurtzite ZnO through decomposition of Zn(OH)2 at various growth temperatures using CBD method. *Opt. Mater.* 46, 292–298. doi:10.1016/j.optmat.2015.04.034

Naz, T., Afzal, A., Siddiqi, H. M., Akhtar, J., Habib, A., Banski, M., et al. (2015). 2-Aminoethanol-mediated wet chemical synthesis of ZnO nanostructures. *Appl. Nanosci.* 5, 425–433. doi:10.1007/s13204-014-0334-1

Onoda, H. (2019). Low temperature phosphoric acid treatment of zinc oxide for nobel white pigments. *Ceram. - Silik.* 63, 291–296. doi:10.13168/cs.2019.0023

Orozco, S., Rivero, M., Montiel, E., and Espino Valencia, J. (2022). Gallium oxides photocatalysts doped with Fe ions for discoloration of rhodamine under UV and visible light. *Front. Environ. Sci.* 10. (Accessed June 9, 2022). doi:10.3389/fenvs.2022.884758

Park, S.-K., and Shin, H. (2014). Effect of HCl and H2SO4 treatment of TiO2 powder on the photosensitized degradation of aqueous rhodamine B under visible light. *J. Nanosci. Nanotechnol.* 14, 8122–8128. doi:10.1166/jnn.2014.9466

Paul, D. R., Gautam, S., Panchal, P., Nehra, S. P., Choudhary, P., Sharma, A., et al. (2020). ZnO-modified g-C3N4: A potential photocatalyst for environmental application. *ACS Omega* 5, 3828–3838. doi:10.1021/acsomega.9b02688

Purcar, V., Rădiţoiu, V., Rădiţoiu, A., Raduly, F. M., Manea, R., Frone, A., et al. (2021). Bilayer coatings based on silica materials and iron (III) phthalocyanine – sensitized TiO2 photocatalyst. *Mater. Res. Bull.* 138, 111222. doi:10.1016/j.materresbull.2021.111222

Qi, K., Cheng, B., Yu, J., and Ho, W. (2017). Review on the improvement of the photocatalytic and antibacterial activities of ZnO. *J. Alloys Compd.* 727, 792–820. doi:10.1016/j.jallcom.2017.08.142

Raha, S., and Ahmaruzzaman, M. (2022). ZnO nanostructured materials and their potential applications: progress, challenges and perspectives. *Nanoscale Adv.* 4, 1868–1925. doi:10.1039/D1NA00880C

Rajamanickam, D., and Shanthi, M. (2014). Photocatalytic degradation of an azo dye Sunset Yellow under UV-A light using TiO2/CAC composite catalysts. *Spectrochimica Acta Part A Mol. Biomol. Spectrosc.* 128, 100–108. doi:10.1016/j.saa.2014.02.126

Rajamanickam, D., Dhatshanamurthi, P., and Shanthi, M. (2015). Preparation and characterization of SeO2/TiO2 composite photocatalyst with excellent performance for sunset yellow azo dye degradation under natural sunlight illumination. *Spectrochimica Acta Part A Mol. Biomol. Spectrosc.* 138, 489–498. doi:10.1016/j.saa.2014.11.070

Shahid, M., Bashir, S., Habib, A., Jamil, A., Afzal, A., Iqbal, N., et al. (2021). Fabrication of silica-supported Al-doped ZnO and its use in the elimination of the toxic organic ingredients from industrial effluents. *ChemistrySelect* 6, 10501–10513. doi:10.1002/slct.202102291

Shahid, M., Bashir, S., Afzal, A., Ibn Shamsah, S. M., and Jamil, A. (2022). Synergistic impacts of composite formation and doping techniques to boost the photocatalytic aptitude of the BiFeO3 nanostructure. *Ceram. Int.* 48, 2566–2576. doi:10.1016/j.ceramint.2021.10.039

Sharma, G., Kumar, A., Sharma, S., Naushad, Mu., Dhiman, P., Vo, D.-V. N., et al. (2020). Fe3O4/ZnO/Si3N4 nanocomposite based photocatalyst for the degradation of dyes from aqueous solution. *Mater. Lett.* 278, 128359. doi:10.1016/j.matlet.2020.128359

Sharwani, A. A., Narayanan, K. B., Khan, M. E., and Han, S. S. (2022). Photocatalytic degradation activity of goji berry extract synthesized silver-loaded mesoporous zinc oxide (Ag@ZnO) nanocomposites under simulated solar light irradiation. *Sci. Rep.* 12, 10017. doi:10.1038/s41598-022-14117-w

Singh, S. C. (2011). Effect of oxygen injection on the size and compositional evolution of ZnO/Zn(OH)2 nanocomposite synthesized by pulsed laser ablation in distilled water. *J. Nanopart. Res.* 13, 4143–4152. doi:10.1007/s11051-011-0359-2

Tănase, M. A., Soare, A. C., Oancea, P., Răducan, A., Mihăescu, C. I., Alexandrescu, E., et al. (2021). Facile *in situ* synthesis of ZnO flower-like hierarchical nanostructures by the microwave irradiation method for multifunctional textile coatings. *Nanomaterials* 11, 2574. doi:10.3390/nano11102574

Varma, K. S., Tayade, R. J., Shah, K. J., Joshi, P. A., Shukla, A. D., Gandhi, V. G., et al. (2020). Photocatalytic degradation of pharmaceutical and pesticide compounds (PPCs) using doped TiO2 nanomaterials: A review. *Water-Energy Nexus* 3, 46–61. doi:10.1016/j.wen.2020.03.008

Wang, Z.-S., Yamaguchi, T., Sugihara, H., and Arakawa, H. (2005). Significant efficiency improvement of the black dye-sensitized solar cell through protonation of TiO2 films. *Langmuir* 21, 4272–4276. doi:10.1021/la050134w

Wang, M., Jiang, L., Kim, E. J., and Hahn, S. H. (2015). Electronic structure and optical properties of Zn(OH)2: LDA+U calculations and intense yellow luminescence. *RSC Adv.* 5, 87496–87503. doi:10.1039/C5RA17024A

Zhang, J., Tian, B., Wang, L., Xing, M., and Lei, J. (2018). *Photocatalysis: Fundamentals, materials and applications*. Singapore: Springer. doi:10.1007/978-981-13-2113-9

Zhang, S., SaeedaKhan, A., Ali, N., Malik, S., Khan, H., et al. (2022). Designing, characterization, and evaluation of chitosan-zinc selenide nanoparticles for visible-light-induced degradation of tartrazine and sunset yellow dyes. *Environ. Res.* 213, 113722. doi:10.1016/j.envres.2022.113722